Root cap cell corpse clearance limits microbial colonization in *Arabidopsis thaliana*

Nyasha M. Charura[1+], Ernesto Llamas[1+], Concetta De Quattro[1], David Vilchez[2,3,4], Moritz K. Nowack[5,6#] and Alga Zuccaro[1#*]

[1] Cluster of Excellence on Plant Sciences (CEPLAS), Institute for Plant Sciences, University of Cologne, D-50674 Cologne, Germany.

[2] Cologne Excellence Cluster for Cellular Stress Responses in Aging-Associated Diseases (CECAD), University of Cologne, 50931 Cologne, Germany.

[3] Center for Molecular Medicine Cologne (CMMC), University of Cologne, 50931 Cologne, Germany.

[4] Faculty of Medicine, University Hospital Cologne, 50931 Cologne, Germany.

[5] Department of Plant Biotechnology and Bioinformatics, Ghent University, 9052 Ghent, Belgium

[6] VIB Center for Plant Systems Biology, 9052 Ghent, Belgium

[#]shared last author

[+]shared first author

*Corresponding author: azuccaro@uni-koeln.de

Abstract

In plants, programmed cell death (PCD) is a fundamental cellular process during development that can also be triggered upon biotic and abiotic stresses. In *Arabidopsis thaliana,* developmental PCD (dPCD) is an integral part of the differentiation process of the root cap, a specialized organ that surrounds the meristematic stem cells. The acquisition of cell death competence in lateral root cap (LRC) cells depends on the root cap-specific transcription factor ANAC033/SOMBRERO (SMB). Cell death is followed by a rapid cell-autonomous corpse clearing process on the root surface, involving the senescence-associated bifunctional nuclease BFN1 downstream of SMB. Based on transcriptomic analyses, we observed the downregulation of *BFN1* during colonization of *A. thaliana* by the beneficial root endophyte *Serendipita indica*, which prompted us to investigate the roles of SMB and BFN1 in fungal accommodation during dPCD. We show that roots of *smb3* mutants, which are deficient in root cap PCD and corpse clearance, are entirely covered by undegraded LRC cell corpses loaded with protein aggregates. The accumulation of uncleared cell corpses promotes intra- and extraradical colonization by *S. indica*, which in turn is sufficient to subsequently clear the cell corpses from the surface of *smb3* roots. Compared to *smb3,* the *bfn1-1* knockout mutant exhibits an attenuated delayed corpse clearance phenotype, but still displays a large amount of protein aggregates and enhances colonization by *S. indica*. These results highlight the importance of root cap differentiation and dPCD in plant-microbe interactions and show that the constant production and clearance of LRC cells, in addition to its function in cap size control, represents a sophisticated physical defense mechanism to prevent microbial colonization in close proximity to meristematic stem cells. Furthermore, we propose a

mechanism by which *S. indica* manipulates dPCD in *A. thaliana* roots by downregulating *BFN1* to promote fungal colonization through delayed clearance of dead cells on the root surface as a potential source of nutrients.

Keywords

Programmed cell death (PCD) / developmental PCD (dPCD) / root cap / lateral root cap (LRC) / SOMBRERO (SMB) / plant-microbe interaction / root colonization / *Serendipita indica* / root cell corpses / root stem cells / BFN1

Introduction

Plant roots elongate by producing new cells in the meristematic tissue at the apical region of root tips. As roots extend further into the soil environment, the newly formed root tissue is naturally exposed to microbial attacks, which poses a challenge to the successful establishment of root systems. However, microbial colonization of the meristematic zone in root tips is rarely detected (Deshmukh *et al.*, 2006, Jacobs *et al.*, 2011). The sensitive tissue of the apical root meristem is surrounded and presumably protected by the root cap, a specialized root organ that orchestrates root architecture, directs root growth based on gravitropism and hydrotropism, and senses environmental stimuli (Kumpf & Nowack, 2015, Moriwaki *et al.*, 2013).

In *Arabidopsis thaliana* (hereafter Arabidopsis), the root cap consists of two distinct tissues: the centrally located columella root cap and the peripherally located lateral root cap (LRC), which flanks both the columella and the entire root meristem (Dolan *et al.*, 1993). A ring of specific stem cells continuously generates both new LRC cells and root epidermis cells (Dolan et al., 1993). However, despite the constant production of LRC cells, the root cap itself does not grow in size but matches the size of the meristem (Fendrych *et al.*, 2014, Barlow, 2002, Kumpf & Nowack, 2015). To maintain size homeostasis, root cap development is a highly regulated process that varies in different plant species. In Arabidopsis, a combination of developmental programmed cell death (dPCD) and shedding of old cells into the rhizosphere has been described (Bennett *et al.*, 2010, Kumpf & Nowack, 2015). The centrally located columella root cap is shed as a cell package into the rhizosphere along with adjacent proximal LRC cells, followed by a PCD process happening in the rhizosphere (Shi *et al.*, 2018, Feng *et al.*, 2022, Huysmans *et al.*, 2018). In contrast, LRC cells in the upper part of the root tip elongate and reach the distal edge of the meristem where they undergo dPCD orchestrated by the root cap-specific transcription factor ANAC33/SOMBRERO (SMB) (Fendrych et al., 2014, Willemsen *et al.*, 2008, Bennett et al., 2010). SMB belongs to a plant-specific family of transcription factors carrying a NAC domain (NAM - no apical meristem; ATAF1 and −2, and CUC2 - cup-shaped cotyledon). In the root cap, SMB directly and indirectly promotes the expression of genes involved in the initiation and execution of LRC cell death, including the senescence-associated nuclease *BFN1* (Huysmans et al., 2018). BFN1 is compartmentalized in the ER and released into the cytoplasm during dPCD to exert its enzymatic activity on nucleic acids in dying cells (Fendrych et al., 2014, Reza et al., 2018). Cytosolic and nuclear DNA and RNA fragmentation, as part of a rapid cell-autonomous corpse clearance on the root surface, is delayed in *bfn1-1* loss-of function mutants (Fendrych et al., 2014). Precise timing of cell death and elimination of LRC cells before they fully enter the root elongation zone is essential for maintaining root cap size and optimal root growth (Fendrych et

al., 2014). Loss of SMB activity results in a delayed cell death, causing LRC cells to enter the elongation zone where they eventually die without expression of dPCD-associated genes in the root cap, such as *BFN1* and *PASPA3* (Olvera-Carrillo et al., 2015). Interestingly, the aberrant cell death of LRC cells in the elongation zone of *smb3* mutants is not followed by corpse clearance, resulting in an accumulation of dead cells along the entire root surface (Fendrych et al., 2014).

Despite its importance in root morphology and plant development, little is known about the impact of impaired dPCD in the root cap on plant-microbe interactions. To address the link between fungal accommodation and plant developmental cell death, we analyzed transcriptomic data and observed downregulation of *BFN1* in Arabidopsis during colonization by *Serendipita indica* (hereafter *S. indica*), a beneficial fungus of the order Sebacinales. As a root endophyte, *S. indica* colonizes the epidermal and cortex layers of a broad range of different plant hosts, conferring various beneficial effects, including plant growth promotion, protection against pathogenic microbes and increased tolerance to abiotic stresses (Boorboori & Zhang, 2022, Mahdi *et al.*, 2022, Fesel & Zuccaro, 2016). The colonization strategy of *S. indica* comprises an initial biotrophic interaction between plant and fungus. Once established in its plant host, *S. indica* enters a growth phase associated with a restricted host cell death that does not, however, diminish the beneficial effects on the plant host. The induction of restricted cell death in host roots is a crucial component of *S. indica* colonization strategy and is accompanied by increased production of fungal hydrolytic enzymes. Although several effector proteins involved in fungal accommodation have been described (Dunken *et al.*, 2022, Weiss *et al.*, 2016), the exact mechanism by which *S. indica* manipulates cell death in plants is still unclear.

Here we show that the bifunctional nuclease *BFN1,* involved in dPCD processes including LRC corpse clearance in roots, is downregulated in Arabidopsis during colonization by *S. indica*, which led us to investigate loss-of-function mutants of BFN1 and its upstream transcriptional regulator SMB. *smb3* mutant plants accumulate uncleared LRC cell corpses, which surround the root and enhance *S. indica* attachment and colonization along the entire root axis, even in the root tip where colonization does not normally occur in wild-type (WT) plants. Furthermore, we show that *S. indica* clears dead LRC cells of *smb3* mutant plants, most likely by degradation and uptake of nutrients from the cell corpses. Similarly, we observe that the *bfn1-1* mutants also enhance fungal colonization, despite a less pronounced delayed corpse clearance phenotype and accumulation of undegraded cells. Both mutants are characterized by the accumulation of protein aggregates in dead and dying cells. Taken together, our data demonstrate that tight regulation of host dPCD and rapid and complete root cap clearance play important roles in restricting fungal colonization. Manipulation of dPCD by downregulating *BFN1* during colonization may therefore provide a means to enhance fungal accommodation and nutrient availability to the fungus.

Results

BFN1, a downstream component of dPCD involved in cell corpse clearance, is downregulated during interaction with *S. indica*

dPCD is the final step of LRC differentiation to maintain root cap organ size in the root tip of Arabidopsis. This process is orchestrated by the transcription factor SMB and executed by its direct and indirect downstream targets, including the nuclease BFN1. To explore the role of root

120 dPCD during *S. indica* accommodation in Arabidopsis, we performed transcriptional analyses to
121 track changes in the expression profile of cell death marker genes during different colonization
122 stages. The major regulator of LRC cell death, the transcription factor *SMB*, showed no changes
123 in expression during fungal colonization (**Fig**. **1A, B**). However, a marked decrease in the
124 expression of the senescence-associated nuclease *BFN1* was observed at 6 days post
125 inoculation (dpi), a time point that correlates with the onset of cell death by *S. indica* in Arabidopsis
126 (**Fig. 1A, B and Fig. S9**). To validate the RNA-Seq analysis, we performed quantitative real time-
127 PCR (qRT-PCR), confirming *BNF1* downregulation at the onset of cell death in *S. indica*-colonized
128 plants (**Fig. 1C**).

129 Induction of dPCD triggers the release of BFN1 from the ER into the cytoplasm, where irreversible
130 fragmentation of cytosolic and nuclear DNA and RNA occurs as part of the clearing of cell corpses
131 (Fendrych et al., 2014). It has previously been shown that the roots of the *bfn1-1* T-DNA insertion
132 KO mutant line exhibit delayed nuclear degradation during corpse clearance (Fendrych et al.,
133 2014, Huysmans et al., 2018) (**Fig. 1D**). Accordingly, staining with Evans blue, a viability dye that
134 penetrates non-viable and damaged cells (Vijayaraghavareddy et al., 2017), showed an increase
135 in cellular remnants on the *bfn1-1* epidermal cell layer at the transition between the elongation
136 and differentiation zones (**Fig. 1E, F**). These results are consistent with the proposed involvement
137 of BFN1 in cell corpse clearance during dPCD in the Arabidopsis root cap.

138 We further characterized the *bfn1-1* mutant with Proteostat, a fluorescent dye that bindsto
139 quaternary protein structures typically found in misfolded and aggregated proteins (Llamas *et al.*,
140 2021). In WT root tips, we have previously observed that protein aggregates accumulate during
141 root differentiation in dying and sloughed columella cell packages but not in young LRC and
142 meristematic cells or healthy differentiated cells (Llamas et al., 2021). While the roots of WT
143 Arabidopsis plants were devoid of Proteostat signal, the *bfn1-1* mutant exhibited staining along
144 the entire root axis. Only the meristematic root tip zone remained free of protein aggregates (**Fig.**
145 **1G, H and Fig. S1**).

146 To investigate the role of BNF1 in *S. indica* root colonization, we quantified extraradical
147 colonization of *S. indica*-inoculated *bfn1-1* and WT seedlings by comparing the staining intensities
148 of the chitin-binding fluorescent marker Alexa Fluor 488 conjugated to Wheat Germ Agglutinin
149 (WGA-AF 488). The *bfn1-1* mutant exhibited significantly stronger staining, indicating higher
150 extraradical colonization than in WT Arabidopsis. (**Fig. 2A-C and Fig. S2**). Quantification of
151 intraradical colonization by qRT-PCR after careful removal of outer fungal hyphae showed
152 increased *S. indica* colonization in the *bfn1-1* mutant at later stages of interaction (**Fig. 2D**).
153 Together, these results suggest that downregulation of *BFN1* during colonization is beneficial for
154 intra- and extraradical fungal accommodation.

155 **SMB is involved in restricting fungal colonization**

156 To better characterize the role of disrupted dPCD in Arabidopsis LRCs, we analyzed the effect of
157 a loss-of-function mutation in the transcription factor SMB, a key element of LRC differentiation
158 and upstream regulator of BFN1 (**Fig. 1D**). The extent of cell death in the *smb3* T-DNA insertion
159 line could be visualized with Evans blue staining, which highlighted the presence of unprocessed
160 LRC cell corpses along the entire surface of *smb3* roots (**Fig. 3A, B**). Proteostat staining revealed

161 an accumulation of protein aggregates in the uncleared dead LRC cells adhering to the roots of
162 *smb3* (**Fig. 3C, D, E**). However, neither Proteostat signal nor Evans blue staining was detected
163 in young LRC cells covering the meristem or in cells underlying the uncleared dead LRC cells in
164 the differentiation zone (**Fig. 3 C, D, E and Fig. S4**). Filter trap analyses confirmed that more
165 protein aggregates were present in *smb3* roots compared to WT roots (**Fig. 3F**). These data
166 indicate that accumulation of protein aggregates occurs in *smb3* LRC cells as they enter the
167 differentiation zone.

168 To assess extracellular fungal colonization, we quantified WGA-AF 488 signal in *S. indica*-
169 inoculated *smb3* and WT seedlings. *S. indica* showed a preferential colonization pattern in the
170 differentiation zone of WT roots and exhibited a significant increase in fungal growth on *smb3*
171 roots along the entire root axis (**Fig. 4A, B**). Interestingly, in *smb3* seedlings *S. indica* also
172 colonized the meristematic zone of the root apex (**Fig. 4A and 5A**), a region normally not
173 associated with microbial colonization (Deshmukh et al., 2006, Jacobs et al., 2011). The
174 intraradical biomass of *S. indica* was also consistently increased in *smb3* compared to WT roots
175 (**Fig. 4C**). Cytological analysis by confocal laser scanning microscopy (CLSM) confirmed that *S.*
176 *indica* does not colonize the root tip of WT plants, but preferentially colonizes the mature parts of
177 the root corresponding to the differentiation zone (**Fig. 5A, C**). In contrast, *S. indica* hyphae were
178 regularly detected around the root tip of *smb3* (**Fig. 5A, B, D**). We also observed that *S. indica*
179 accommodates in cells that are subject to cell death and protein aggregation (**Fig. 5B, D, E**).
180 Thus, these data indicate that uncleared LRC cell corpses in *smb3* appear to function like a
181 scaffold for fungal colonization even at the root tip and that continuous clearance of root cap cells
182 is likely a mechanism to prevent microbial colonization of the root tip.

183 To assess whether *S. indica* is able to digest the accumulating root cap cell corpses in the *smb3*
184 mutant, we compared Evans blue staining for cell death of colonized and uncolonized roots. While
185 mock-inoculated *smb3* roots displayed an accumulation of Evans blue stained LRC cell corpses
186 along the roots, *smb3* roots colonized with *S. indica* were cleared of the excess dead LRC cells
187 (**Fig. 5F and Fig. S9**). These results suggest that a surplus of cells corpses in *smb3* promotes
188 colonization by *S. indica*.

189 **Cell non-autonomous activation of cell death by *S. indica***

190 In Arabidopsis WT roots, dPCD execution and corpse clearance orchestrated by the transcription
191 factor SMB and the nuclease BFN1 prevents unintended accumulation of LRC cell corpses
192 upstream of the meristem (Fendrych et al., 2014). Based on the observation that *S. indica*
193 downregulates *BFN1*, we hypothesized that such downregulation leads to a reduced rate of cell
194 corpse clearance in WT roots, which positively affects *S. indica* by serving as potential additional
195 sources of nutrients. To test this hypothesis, we performed cytological analyses with WT
196 Arabidopsis roots inoculated with *S. indica*. Proteostat staining occurred along the differentiation
197 zone of the entire root axis during *S. indica* colonization, while Evans blue staining was most
198 evident in the young differentiated tissue near the root tip (**Fig. 6A, B and Fig. S6**). Based on
199 measurements from the root tip to the first root hairs, it was found that WT roots inoculated with
200 *S. indica* had a significantly shorter elongation zone (**Fig. 6A and Fig. S5, S6**). The detection of
201 cell death *via* Evans blue staining at the transition between elongation and differentiation zone,
202 where the fungus is typically absent, indicates a systemic activation of cell death in this part of

203 the root. In addition, we found that the pattern highlighted by Evans blue and Proteostat staining
204 in *S. indica*-colonized WT Arabidopsis roots resembled the phenotype of mock-inoculated *bfn1-1*
205 roots (**Fig. 6A and Fig. S6, S8**). For instance, we observed an accumulation of dead cells just
206 above the meristem boundaries of *bfn1-1* as well as a shorter elongation zone (**Fig. 6A and Fig.**
207 **S5, S8**). At this stage, we cannot discriminate whether the observed shorter elongation zone is
208 due to an effect on cell division or cell elongation or due to a systemic effect on the whole root tip
209 zone leading to an earlier onset of the root hair zone. Nevertheless, our results suggest that *S.*
210 *indica* affects dPCD by reducing LRC clearance in Arabidopsis root caps in a non-cell
211 autonomous manner.

212 To determine whether other beneficial microbes affect dPCD by downregulating *BFN1*, we
213 analyzed the transcriptional response of Arabidopsis roots colonized by *S. vermifera*, an
214 endophytic fungus closely related to *S. indica*, and two bacterial synthetic communities
215 (SynComs) isolated from Arabidopsis or *Hordeum vulgare* (Mahdi et al., 2022). *BFN1* levels were
216 reduced in WT Arabidopsis roots during all three microbial interactions (**Fig. 7**). Furthermore,
217 similar to *S. indica*, the interaction of *S. vermifera* with Arabidopsis led to an induction of cell death
218 in young differentiated root tissues and to a shorter elongation zone (**Fig. S5, S7**). These results
219 suggest that beneficial microbes may have evolved the ability to manipulate dPCD and root cap
220 turnover to increase symbiotic colonization (**Fig. 8**).

221 **Discussion**

222 **Impaired dPCD affects plant-microbe interactions**

223 Developmental cell death in plants and animals is a process critical for differentiation and
224 homeostasis. As new tissue grows, old tissue must be disposed of to maintain healthy
225 homeostasis at cellular and systemic levels. Examples of dPCD in plants can be found in xylem
226 development, where controlled cell death forms cavities for water transport or in lateral root
227 formation, which is facilitated by restricted cell death in cell layers above developing root primordia
228 (Escamez *et al.*, 2020, Heo *et al.*, 2017). As a plant organ that continuously produces new tissues
229 but maintains a fixed size, the root cap is characterized by high cellular turnover (Kumpf and
230 Nowack, 2015). Such cellular turnover in LRCs of Arabidopsis roots is controlled by the
231 transcription factor SMB and downstream by the nuclease BFN1 (Fendrych et al., 2014). Despite
232 its importance in plant health and development, little attention has been paid to the influence of
233 dPCD on accommodation of microbes and vice versa.

234 In this study, we investigated the functional link between dPCD processes and microbial
235 accommodation by characterizing *smb3* and *bfn1-1* Arabidopsis mutants during fungal
236 interaction. We found that interference with dPCD and corpse clearance in the root cap, has
237 implications for the entire root system, with some nuanced differences. While *smb3* roots are
238 sheathed with dead, uncleared LRC cells, the underlying epidermal cells do not seem to be
239 affected (**Fig. S4**). In *bfn1-1* roots we observed an attenuated uncontrolled cell death phenotype
240 in the differentiation zone. Here, it remains unclear whether these cells originate from the root cap
241 or are epidermal cells damaged by delayed LRC clearance (**Fig. 1E, F and 3A, B**). Both mutations
242 are characterized by increased protein aggregation. However, while the presence of protein
243 aggregates in *smb3* is restricted to LRC cell corpses and is consistent with Evans blue staining,

244 the epidermal cell layer of *bfn1-1* is littered with aggregates along the root axis, regardless of the
245 occurrence of cell death. These data suggest that BFN1 activity is not limited to its proposed
246 function in eliminating LRC cell corpses in the root tip. We hypothesize that BFN1 nuclease activity
247 may be involved in the production of active nucleotide metabolites that activate signaling
248 pathways regulating dPCD and cell corpse clearance. The fact that small active metabolites can
249 induce cell death has recently been shown (Yu *et al.*, 2022). In plants, the Toll/interleukin-1
250 receptor (TIR) domains of nucleotide-binding leucine rich repeat (NLR) immunoreceptors possess
251 NADase enzymatic activity, as well as 2′,3′-cAMP/cGMP synthetases activity by hydrolyzing
252 RNA/DNA (Duxbury *et al.*, 2020, Yu et al., 2022). While NADase activity is not sufficient to induce
253 plant immune responses, mutations that specifically disrupt synthetase activity abolish TIR-
254 mediated cell death in *Nicotiana benthamiana*, demonstrating that cNMPs (cyclic nucleotide
255 monophosphates) play an important role in TIR immune signaling. Also it was shown that the
256 combined activity of two fungal apoplastic enzymes, the ecto-5'-nucleotidase E5NT and the
257 nuclease NucA from *S. indica*, leads to the production of deoxyadenosine (dAdo), a metabolite
258 that, upon uptake, triggers a TIR-NLR-modulated plant cell death (Dunken et al., 2022). These
259 results suggest that the DNAse activity of BFN1 may be involved in the production of small active
260 metabolites in the plant that affect plant-microbe interactions and cell death. These results
261 suggest that the DNAse activity of BFN1 may be involved in the production of small active
262 metabolites in the plant that affect plant-microbe interactions and cell death. Differential
263 modulation of potential infochemicals in the *bfn1-1* mutant could therefore delay cellular damage
264 signaling and cause protein aggregation. A hypothesis that should be further analyzed by
265 metabolomic and proteomic approaches.

266 To investigate the role of dPCD in the root cap during interaction with plant microbes, we assayed
267 intra- and extraradical colonization with the endophytic fungus *S. indica* in *bfn1-1* and *smb3*
268 mutants (**Fig. 2 and 4**). Both approaches show that attenuation or loss of corpse clearance in the
269 root cap increases fungal colonization. Because of the observation that *S. indica* is able to clear
270 the LRC cell corpses on *smb3* roots, we hypothesize that the uncleared LRC cells provide an
271 additional source of nutrients that promote overall fungal growth. Whether production of the
272 above-described dAdo by *S. indica* potentially influences dPCD remains to be tested.

273 In WT plants, the root tip is usually free of microbial colonization (Deshmukh et al., 2006, Jacobs
274 et al., 2011). Interestingly, we detected significant fungal colonization around the root tip of *smb3*,
275 but not *bfn1-1* or WT plants. Cytological analyses have shown that *S. indica* grows in detached,
276 dead cell packages of LRC and columella cells, but rarely in WT root tips (Dunken et al., 2022,
277 Deshmukh et al., 2006). The phenotype of *smb3* shows resemblance to the human skin disease
278 hyperkeratosis. In healthy human skin, a pool of stem cells produces layers of cells that divide,
279 differentiate, die, and are shed. Such developmental programs form a physical and dynamic
280 barrier. When microbes attempt to establish themselves in the skin, they are consistently removed
281 by skin exfoliation (Dettmer, 2021). Patients with hyperkeratosis show an accumulation of dead
282 cells on the outer layer of their skin, making it more susceptible to microbial infection (Cheng *et*
283 *al.*, 1992). Our results suggest that root cap turnover in Arabidopsis, similar to human skin
284 turnover, may be a sophisticated physical mechanism to prevent or reduce intracellular microbial
285 colonization near the root meristematic tissue. In contrast, despite the delayed clearance

286 phenotype, *bfn1-1* does not appear to accumulate additional root cap layers and thus prevent
287 fungal accommodation in the root tip.

288 Together, we demonstrate that proper root cap development, including cell death and cell
289 clearance, influences plant-microbe interactions and is important for restricting microbial
290 colonization in the root tip (**Fig. 8**).

291 **Microbial manipulation of developmental cell death**

292 The root cap is thought to be associated with protection of the underlying meristematic stem cells
293 (Kumar & Iyer-Pascuzzi, 2020). Previous studies have highlighted the importance of the root cap
294 in plant-microbe interactions, for example the physical removal of the root cap in maize plants
295 leads to increased colonization of the root tip by *Pseudomonas fluorescens* (Humphris *et al.*,
296 2005). However, little is known about the impact of microbial colonization on plant dPCD. Here,
297 we propose that microbes affect dPCD and corpse clearance in the root cap of Arabidopsis by
298 downregulating the nuclease *BFN1*.

299 Many features of the root phenotype induced by *S. indica* colonization show striking similarities
300 to the root phenotype of *bfn1-1* mutant. These similarities include the cell death pattern in young,
301 differentiated root tissue and the shortened elongation zone, which we hypothesize are remnants
302 of delayed LRC corpse clearance and promote fungal growth by providing additional nutrients.
303 Concerning the increased protein aggregation in *bfn1-1* and *S. indica*-colonized WT roots, it is
304 still unknown whether *S. indica*-induced protein aggregation is directly or indirectly linked to *BFN1*
305 downregulation or whether other components contribute to the similarities in phenotype. However,
306 the similarities in *bfn1-1* and *S. indica* colonization phenotypes suggest that the biphasic
307 colonization strategy of *S. indica* in Arabidopsis may be related to the temporal downregulation of
308 the nuclease activity of BFN1 and thus to the manipulation of dPCD in the root cap.

309 However, the mechanism controlling *BFN1* downregulation remains to be investigated because it
310 is unclear whether an active interference by fungal effector proteins or signaling molecules or a
311 systemic response of Arabidopsis occurs in the presence of *S. indica*. Previous studies have
312 shown that *S. indica* preferentially colonizes roots in the mature differentiation zone, but we
313 observed a cell death pattern in the young differentiation tissue near the root tip. Therefore, we
314 suggest that active downregulation by effector proteins is unlikely due to the spatial separation of
315 the two zones (**Fig. 6**). In addition, we have shown that other beneficial microbes such as the
316 closely related fungus *Serendipita vermifera* and two synthetic bacterial communities (SynComs)
317 isolated from Arabidopsis and *Hordeum vulgare* (Mahdi et al., 2022) also downregulate *BFN1*
318 during Arabidopsis colonization. These results highlight the possibility of a conserved systemic
319 response of Arabidopsis to beneficial microbes that involves the downregulation of *BFN1* to
320 facilitate symbiotic interactions. It remains to be clarified whether this applies only to beneficial or
321 also to pathogenic microbes. However, unlike *SMB*, *BFN1* expression in Arabidopsis is not
322 restricted to the root cap. Therefore, future studies should clarify whether downregulation of
323 senescence-associated *BFN1* by microbes occurs locally in the root cap as part of SMB-induced
324 cell death or as part of general cell death processes throughout the root. Further questions remain
325 about the signaling capacities of BFN1 nuclease activity via infochemicals production and its
326 potential activity to regulate plant proteostasis and/or microbe interactions.

327 In conclusion, our data indicate that tight regulation of host dPCD and proper root cap clearance
328 play an important role in restricting fungal colonization. However, the microbes may have evolved
329 signaling pathways to manipulate dPCD and root cap turnover, to promote symbiotic colonization
330 in dying root cells (**Fig. 8**).

331 **Materials and methods**

332 **Fungal strains and growth conditions**

333 Fungal experiments were performed with *Serendipita indica* strain DSM11827 (German
334 Collection of Microorganisms and Cell Cultures, Braunschweig, Germany). *S. indica* was grown
335 on complete medium (CM) containing 2% (w/v) glucose and 1.5 % (w/v) agar (Hilbert et al., 2012).
336 Fungal material was grown at 28 °C in the dark for 4 weeks before spore preparation.

337 For additional experiments, fungal strain *Serendipita vermifera* (MAFF305830) was used and
338 grown on MYP medium containing 1.5% agar at 28 °C in darkness for 3 weeks before mycelium
339 preparation for root inoculation.

340 **Plant material and growth conditions**

341 Seeds of *Arabidopsis thaliana* ecotype Columbia 0 (Col-0) and T-DNA insertion mutants (*bfn1-1*
342 [GK-197G12] and *smb3* [SALK_143526C]) in Col-0 background were used for experiments.

343 Seeds were surface sterilized in 70% ethanol for 15 min and 100% ethanol for 12 min, stratified
344 at 4°C in the dark for 3 days and germinated and grown on ½ MS medium (Murashige-Skoog
345 Medium, with vitamins, pH 5.7) containing 1% (w/v) sucrose and 0.4 %(w/v) Gelrite under short -
346 day conditions (8 h light, 16 h dark) with 130 µmol $m^{-2\ s-1}$ light and 22°C/18 °C.

347 **Fungal inoculation**

348 One-week-old seedlings were transferred to 1/10 PNM (Plant Nutrition Medium, pH 5.7) plates
349 without sucrose, using 15 to 20 seedlings per plate. Under sterile conditions, chlamydospores of
350 *S. indica* were scraped from solid CM plates in 0.002% Tween water (Roth), washed two times
351 with ddH_2O and pipetted in a volume of 2ml directly on plant roots and surrounding area in a
352 concentration of $5x10^5$ per plate. ddH_2O was used for inoculation of mock plants. Unless otherwise
353 indicated, plants were treated using this inoculation protocol. Where indicated we also incoulated
354 Arabidopsis seeds with *S. indica*. For this case, Arabidopsis seeds were surface sterilized,
355 incubated with fungal spore solution at $5x10^5$ concentration for 1 hour and plated on ½ MS plates
356 (without sucrose).

357 For *S. vermifera* inoculation, mycelium was scrapped from plates in ddH_2O, washed and added
358 to Arabidopsis roots in a volume of 1ml of a stock solution of 1 g / 50 ml.

359 **Evans blue staining**

360 For the visualization of cell death in Arabidopsis roots a modified protocol by (Vijayaraghavareddy
361 *et al.*, 2017) was used. Roots were washed three times in ddH_2O to remove lose external fungal
362 growth and then stained for 15 minutes in 2 mM Evans blue (Sigma-Aldrich) dissolved in 0.1 M
363 $CaCl_2$ pH 5.6. Following, roots were washed extensively with ddH_2O for 1 hour and a Leica M165
364 FC microscope was used for imaging.

365 To quantify Evans blue staining intensity, ImageJ was used to invert the pictures, draw out
366 individual roots and measure and compare mean grey values.

367 **Extraradical colonization assays**

368 To quantify extraradical colonization of *S. indica* on Arabidopsis, seed inoculated plants were
369 grown for 10 days. Inoculated and mock-treated seedlings were stained directly on plate by
370 pipetting 2 ml of 1X PBS solution containing Alexa Fluor 488 conjugated with Wheat Germ
371 Agglutinin (WGA-AF 488, Invitrogen). After 2 min of incubation, the roots were washed twice on
372 the plate with 1X PBS solution. The stained seedlings were transferred to a fresh ½ MS plate and
373 scanned with an Odyssey M Imaging System (LI-COR Biosciences) using brightfield and Alexa
374 Fluor 488 channel. Quantification of WGA-AF 488 fluorescence was performed using
375 EmpiriaStudio Software (LI-COR Biosciences).

376 **RNA extraction (intraradical colonization assay)**

377 For RNA extraction to measure intraradical colonization, plants were harvested at three time
378 points around 7, 10 and 14 dpi. The roots were extensively wash with ddH_2O and tissue paper
379 was used carefully wipe off external fungal colonization. The roots were shock frozen in liquid
380 nitrogen and fungal and plant RNA was extracted with TRIzol (Invitrogen, Thermo Fisher
381 Scientific, Schwerte, Germany). After a DNase I (Thermo Fisher Scientific) treatment according
382 to the manufacturer's instructions to remove DNA, RNA was synthesized to cDNA using the
383 Fermentas First Strand cDNA Synthesis Kit (Thermo Fisher Scientific).

384 **Quantitative RT-PCR analysis**

385 The quantitative real time-PCR (qRT-PCR) was performed using a CFX connect real time system
386 (BioRad) with the following program: 95 °C 3min, 95 °C 15s, 59 °C 20s, 72 °C 30s, 40 cycles and
387 melting curve analysis. Relative expression was calculated using the $2^{-\Delta\Delta CT}$ method (Livak and
388 Schmittgen 2001). qRT-PCR primers can be found in Table S1.

389 **Filter trap analyses**

390 Filter trap assays were performed as previously described (Llamas *et al.*, 2022, Llamas et al.,
391 2021). Protein extracts were obtained using native lysis buffer (300 mM NaCl, 100 mM HEPES
392 pH 7.4, 2 mM EDTA, 2% Triton X-100) supplemented with 1x plant protease inhibitor (Merck).
393 Cell debris was removed by several centrifugation steps at 8,000 x *g* for 10 min at 4 °C. The
394 supernatant was separated, and protein concentration determined using the Pierce BCA Protein
395 Assay Kit (Thermo Fisher). A cellulose acetate membrane filter (GE Healthcare Life Sciences)
396 and 3 filter papers (BioRad, 1620161) were immersed in 1x PBS and placed in a slot blot
397 apparatus (Bio-Rad) connected to a vacuum system. The membrane was equilibrated by 3
398 washes with equilibration buffer (native buffer containing 0.5% SDS). 300, 200 and 100 µg of the
399 protein extract were mixed with SDS at a final concentration of 0.5% and filtered through the
400 membrane. The membrane was then washed with 0.2% SDS and blocked with 3% BSA in TBST
401 for 30 minutes, followed by 3 washes with TBST. Incubation was performed with anti-polyQ
402 [1:1000] (Merck, MAB1574). The membrane was washed 3 times for 5 minutes and incubated
403 with secondary antibodies in TBST 3% BSA for 30 minutes. The membrane was developed using
404 the Odyssey M Imaging System (LI-COR Biosciences). Extracts were also analyzed by SDS-

405 PAGE and western blotting against anti-Actin [1:5000] (Agrisera, AS132640) to determine loading
406 controls.

407 **Confocal laser scanning microscopy (CLSM) and Proteostat staining quantification**

408 CLSM images were acquired using either the FV1000 confocal laser scanning microscope
409 (Olympus) or a Meta 710 confocal microscope with laser ablation 266 nm (Zeiss). All images
410 were acquired using the same parameters between experiments. Excitation of WGA-AF 488
411 was done with an argon laser at 488 nm and the emitted light was detected with a hybrid
412 detector at 500-550 nm. Proteostat was excited at 561 nm and the signal was detected
413 between 590-700 nm. Hoechst was excited with a diode laser at 405 nm and the emitted
414 light was detected with a hybrid detector at 415-460 nm.
415
416 **Proteostat staining**
417
418 For the detection of aggregated proteins, we used the Proteostat Aggresome detection kit (Enzo
419 Life Sciences). Seedlings were stained according to the manufacturer's instructions. Seedlings
420 were incubated with permeabilizing solution (0.5% Triton X-100, 3 mM EDTA, pH 8.0) for 30
421 minutes at 4ºC with gentle shaking. The seedlings were washed twice with 1X PBS. Then the
422 plants were incubated in the dark with 1x PBS supplemented with 0.5 µl/ml Proteostat and 0.5
423 µl/ml Hoechst 33342 (nuclear stain) for 30 minutes at room temperature. Finally, the seedlings
424 were washed twice with 1x PBS and mounted on a slide for CLSM analysis or in mounted in
425 fresh MS plates for LI-COR analysis. Quantification of Proteostat fluorescence was performed
426 using Fiji software or EmpiriaStudio Software (LI-COR Biosciences).
427

428 **Transcriptomic analysis**

429 Arabidopsis Col-0 roots were inoculated with *S. indica*. Arabidopsis roots were harvested from
430 mock plants and inoculated plants at four different time points after inoculation: 3, 6 and 10 dpi.
431 Three biological replicates were considered for each condition. The RNA-seq libraries were
432 generated and sequenced at US Department of Energy Joint Genome Institute (JGI) under a
433 project proposal (Proposal ID: 505829) (Zuccaro & Langen, 2020). For each sample, stranded
434 RNASeq libraries were generated and quantified by qRT-PCR. RNASeq libraries were sequenced
435 with Illumina sequencer. Raw reads were filtered and adapter sequences were trimmed using the
436 JGI QC pipeline. Filtered reads from each library were aligned to the Arabidopsis reference
437 genome (TAIR9) using HISAT2 (Kim *et al.*, 2015) and the reads mapped to each gene were
438 estimated using featureCounts (Liao *et al.*, 2014) Differential gene expression analysis was
439 performed using the R package DESeq2 (Love *et al.*, 2014). Genes having aFDR adjusted p-
440 value < 0.05 were considered as differentially expressed genes (DEGs).

441 **CONTRIBUTIONS**

442 Conceptualization: NC, EL, MN, AZ

443 Methodology: NC, EL, CDC

Investigation: NC, EL, CDC, DV, MN, AZ

Visualization: NC, EL, CDC

Funding acquisition: MN, AZ

Project administration: AZ

Supervision: MN, AZ

Writing original draft: EL, NC, AZ

Writing review and editing: All authors

Acknowledgements

We thank the imaging facilities of CECAD (A. Schauss and C. Jüngst) and CEPLAS (P.S. Tan) for their assistance with CLSM. We thank Lisa Madhi for conducting the experiments and providing the samples used for the RNA-seq analysis. We further would like to thank Yu Zhang, Sravanthi Tejomurthula, Daniel Peterson, Vivian Ng & Igor Grigoriev and their work performed in the work proposal (10.46936/10.25585/60001292) conducted by the U.S. Department of Energy Joint Genome Institute (https://ror.org/04xm1d337), a DOE Office of Science User Facility, is supported by the Office of Science of the U.S. Department of Energy operated under Contract No. DE-AC02-05CH11231.

Funding

German Research Foundation (DFG) - Excellence Strategy of the Federal Republic of Germany - EXC-2048/1 - project ID 390686111 (CEPLAS) (NC, EL, AZ)

German Research Foundation (DFG) - SFB-1403-414786233 (AZ)

German Research Foundation (DFG) - German Excellence Strategy-CECAD, EXC 2030-390661388 (DV).

Competing interests:

The Authors declare that they have no competing interests.

Data and materials availability:

All data are available in the main text or supplementary materials. Additional data/materials for this paper can be requested from the authors.

References

~~Balint-Kurti, P. (2019) The plant hypersensitive response: concepts, control and consequences. *Mol Plant Pathol,* **20,** 1163-1178.~~

Barlow, P. W. (2002) The Root Cap: Cell Dynamics, Cell Differentiation and Cap Function. *Journal of Plant Growth Regulation,* **21,** 261-286.

Bennett, T., van den Toorn, A., Sanchez-Perez, G. F., Campilho, A., Willemsen, V., Snel, B.*, et al.* (2010) SOMBRERO, BEARSKIN1, and BEARSKIN2 regulate root cap maturation in Arabidopsis. *Plant Cell,* **22,** 640-654.

Boorboori, M. R. and Zhang, H. Y. (2022) The Role of Serendipita indica (Piriformospora indica) in Improving Plant Resistance to Drought and Salinity Stresses. *Biology (Basel),* **11**.

Cannesan, M. A., Gangneux, C., Lanoue, A., Giron, D., Laval, K., Hawes, M.*, et al.* (2011) Association between border cell responses and localized root infection by pathogenic Aphanomyces euteiches. *Ann Bot,* **108,** 459-469.

Cheng, J., Syder, A. J., Yu, Q. C., Letai, A., Paller, A. S. and Fuchs, E. (1992) The genetic basis of epidermolytic hyperkeratosis: a disorder of differentiation-specific epidermal keratin genes. *Cell,* **70,** 811-819.

Deshmukh, S., Huckelhoven, R., Schafer, P., Imani, J., Sharma, M., Weiss, M.*, et al.* (2006) The root endophytic fungus Piriformospora indica requires host cell death for proliferation during mutualistic symbiosis with barley. *Proc Natl Acad Sci U S A,* **103,** 18450-18457.

Dettmer, P. (2021) *Immune: The new book from Kurzgesagt - a gorgeously illustrated deep dive into the immune system*. Hodder & Stoughton.

Dolan, L., Janmaat, K., Willemsen, V., Linstead, P., Poethig, S., Roberts, K.*, et al.* (1993) Cellular organisation of the Arabidopsis thaliana root. *Development,* **119,** 71-84.

Dunken, N., Widmer, H., Balcke, G. U., Straube, H., Langen, G., Charura, N. M.*, et al.* (2022) A fungal endophyte-generated nucleoside signal regulates host cell death and promotes root colonization. *bioRxiv***,** 2022.2003.2011.483938.

Duxbury, Z., Wang, S., MacKenzie, C. I., Tenthorey, J. L., Zhang, X., Huh, S. U.*, et al.* (2020) Induced proximity of a TIR signaling domain on a plant-mammalian NLR chimera activates defense in plants. *Proc Natl Acad Sci U S A,* **117,** 18832-18839.

Escamez, S., Andre, D., Sztojka, B., Bollhoner, B., Hall, H., Berthet, B.*, et al.* (2020) Cell Death in Cells Overlying Lateral Root Primordia Facilitates Organ Growth in Arabidopsis. *Curr Biol,* **30,** 455-464 e457.

Fendrych, M., Van Hautegem, T., Van Durme, M., Olvera-Carrillo, Y., Huysmans, M., Karimi, M.*, et al.* (2014) Programmed cell death controlled by ANAC033/SOMBRERO determines root cap organ size in Arabidopsis. *Curr Biol,* **24,** 931-940.

Feng, Q., De Rycke, R., Dagdas, Y. and Nowack, M. K. (2022) Autophagy promotes programmed cell death and corpse clearance in specific cell types of the Arabidopsis root cap. *Curr Biol,* **32,** 2110-2119 e2113.

Fesel, P. H. and Zuccaro, A. (2016) Dissecting endophytic lifestyle along the parasitism/mutualism continuum in Arabidopsis. *Curr Opin Microbiol,* **32,** 103-112.

Heo, J. O., Blob, B. and Helariutta, Y. (2017) Differentiation of conductive cells: a matter of life and death. *Curr Opin Plant Biol,* **35,** 23-29.

519 Humphris, S. N., Bengough, A. G., Griffiths, B. S., Kilham, K., Rodger, S., Stubbs, V.*, et al.* (2005)
520 Root cap influences root colonisation by Pseudomonas fluorescens SBW25 on maize.
521 *FEMS Microbiol Ecol,* **54,** 123-130.
522 Huysmans, M., Buono, R. A., Skorzinski, N., Radio, M. C., De Winter, F., Parizot, B.*, et al.* (2018)
523 NAC Transcription Factors ANAC087 and ANAC046 Control Distinct Aspects of
524 Programmed Cell Death in the Arabidopsis Columella and Lateral Root Cap. *Plant Cell,*
525 **30,** 2197-2213.
526 Jacobs, S., Zechmann, B., Molitor, A., Trujillo, M., Petutschnig, E., Lipka, V.*, et al.* (2011) Broad-
527 spectrum suppression of innate immunity is required for colonization of Arabidopsis roots
528 by the fungus Piriformospora indica. *Plant Physiol,* **156,** 726-740.
529 Kim, D., Langmead, B. and Salzberg, S. L. (2015) HISAT: a fast spliced aligner with low memory
530 requirements. *Nat Methods,* **12,** 357-360.
531 Kumar, N. and Iyer-Pascuzzi, A. S. (2020) Shedding the Last Layer: Mechanisms of Root Cap
532 Cell Release. *Plants (Basel),* **9**.
533 Kumpf, R. P. and Nowack, M. K. (2015) The root cap: a short story of life and death. *J Exp Bot,*
534 **66,** 5651-5662.
535 Liao, Y., Smyth, G. K. and Shi, W. (2014) featureCounts: an efficient general purpose program
536 for assigning sequence reads to genomic features. *Bioinformatics,* **30,** 923-930.
537 Llamas, E., Koyuncu, S., Lee, H. J., Gutierrez-Garcia, R., Dunken, N., Charura, N.*, et al.* (2022)
538 Chloroplast protein import determines plant proteostasis and retrograde signaling.
539 *bioRxiv***,** 2022.2003.2019.484971.
540 Llamas, E., Torres-Montilla, S., Lee, H. J., Barja, M. V., Schlimgen, E., Dunken, N.*, et al.* (2021)
541 The intrinsic chaperone network of Arabidopsis stem cells confers protection against
542 proteotoxic stress. *Aging Cell,* **20,** e13446.
543 Love, M. I., Huber, W. and Anders, S. (2014) Moderated estimation of fold change and dispersion
544 for RNA-seq data with DESeq2. *Genome Biol,* **15,** 550.
545 Mahdi, L. K., Miyauchi, S., Uhlmann, C., Garrido-Oter, R., Langen, G., Wawra, S.*, et al.* (2022)
546 The fungal root endophyte Serendipita vermifera displays inter-kingdom synergistic
547 beneficial effects with the microbiota in Arabidopsis thaliana and barley. *ISME J,* **16,** 876-
548 889.
549 Moriwaki, T., Miyazawa, Y., Kobayashi, A. and Takahashi, H. (2013) Molecular mechanisms of
550 hydrotropism in seedling roots of Arabidopsis thaliana (Brassicaceae). *Am J Bot,* **100,** 25-
551 34.
552 Olvera-Carrillo, Y., Van Bel, M., Van Hautegem, T., Fendrych, M., Huysmans, M., Simaskova, M.*,*
553 *et al.* (2015) A Conserved Core of Programmed Cell Death Indicator Genes Discriminates
554 Developmentally and Environmentally Induced Programmed Cell Death in Plants. *Plant*
555 *Physiol,* **169,** 2684-2699.
556 Shi, C. L., von Wangenheim, D., Herrmann, U., Wildhagen, M., Kulik, I., Kopf, A.*, et al.* (2018)
557 The dynamics of root cap sloughing in Arabidopsis is regulated by peptide signalling. *Nat*
558 *Plants,* **4,** 596-604.
559 Vijayaraghavareddy, P., Adhinarayanreddy, V., Vemanna, R. S., Sreeman, S. and Makarla, U.
560 (2017) Quantification of Membrane Damage/Cell Death Using Evan's Blue Staining
561 Technique. *Bio Protoc,* **7,** e2519.

562 Weiss, M., Waller, F., Zuccaro, A. and Selosse, M. A. (2016) Sebacinales - one thousand and
563 one interactions with land plants. *New Phytol,* **211,** 20-40.
564 Willemsen, V., Bauch, M., Bennett, T., Campilho, A., Wolkenfelt, H., Xu, J.*, et al.* (2008) The NAC
565 domain transcription factors FEZ and SOMBRERO control the orientation of cell division
566 plane in Arabidopsis root stem cells. *Dev Cell,* **15,** 913-922.
567 Yu, D., Song, W., Tan, E. Y. J., Liu, L., Cao, Y., Jirschitzka, J.*, et al.* (2022) TIR domains of plant
568 immune receptors are 2',3'-cAMP/cGMP synthetases mediating cell death. *Cell,* **185,**
569 2370-2386 e2318.
570 Zuccaro, A. and Langen, G. (2020) Host-specific regulation of effector gene expression in
571 mutualistic root endophytic fungi (Proposal ID: 505829). JGI Award

572
573
574
575
576
577
578
579
580
581
582
583
584
585
586
587
588
589
590
591
592
593

Figures and descriptions

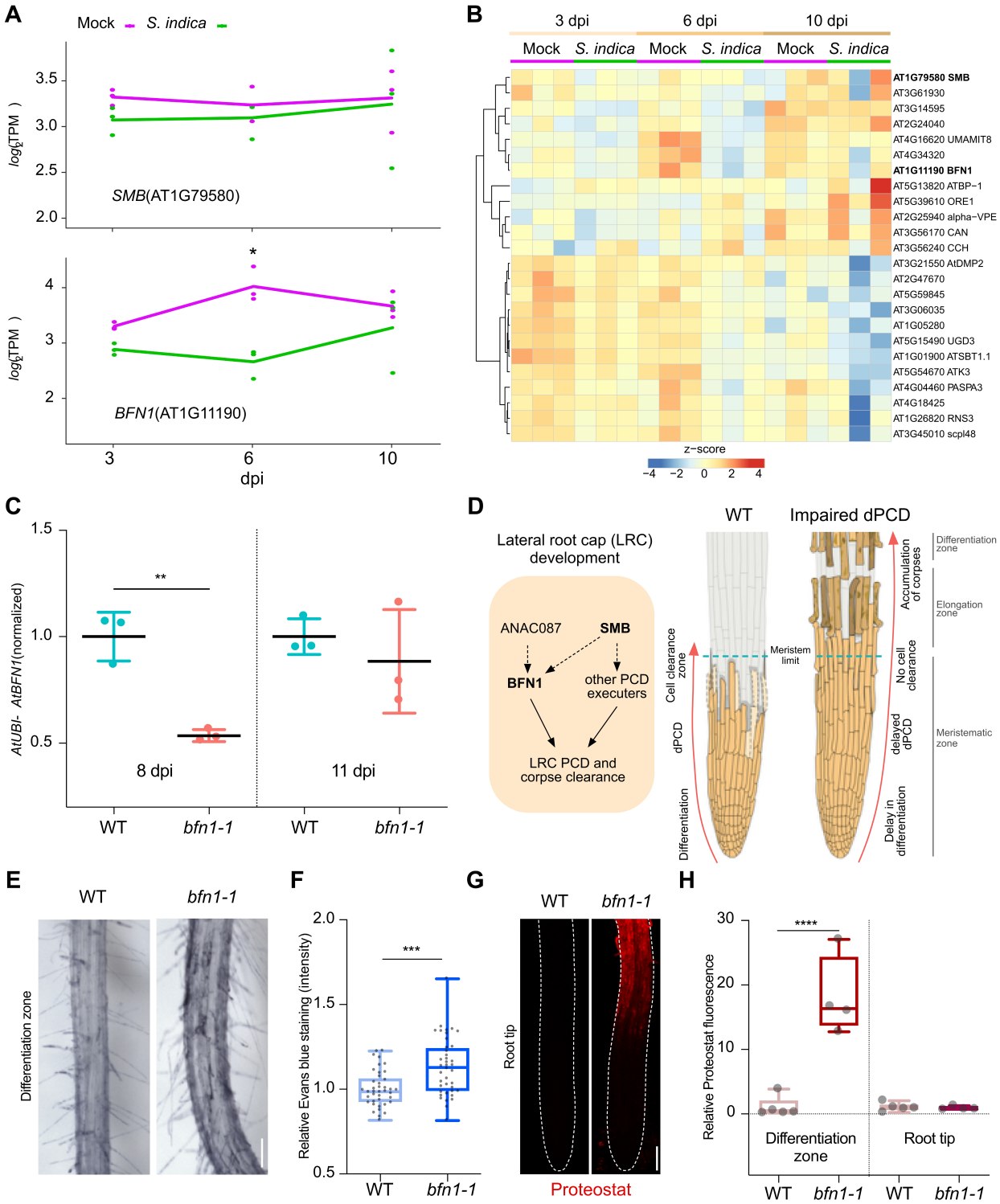

Figure 1. *BFN1* is downregulated during interaction with *S. indica*. (A) Expression profiles of *SMB* and *BFN1* genes in Arabidopsis roots mock-treated or inoculated with *S. indica* at 3, 6 and 10 dpi. The $\log_2$-transformed TPM values are shown and the lines indicate the average expression values among the 3 biological replicates. Asterisk indicates significantly different expression (adjusted p-value < 0.05) (B) The heat map shows the expression values (TPM) of Arabidopsis dPCD marker genes with at least an average of 1 TPM across Arabidopsis roots mock-treated or inoculated with *S. indica* at 3, 6 and 10 dpi. The TPM expression values are $\log_2$ transformed and row-scaled. Genes are clustered using spearman correlation as distance measure. The dPCD gene markers were previously defined in (Olvera-Carrillo et al., 2015). (C) *BFN1* expression in WT Arabidopsis during *S. indica* colonization at 8 and 11 dpi. RNA was isolated from 3 biological replicates for quantitative RT-PCR analysis, comparing *BFN1* expression with an Arabidopsis ubiquitin marker gene. (D) Schematic representation of lateral root cap (LRC) development in WT and in mutant plants impaired in dPCD. (E) Representative images of the differentiation zone of 14-day-old WT and *bfn1-1* roots, stained with Evans blue. Scale indicates 100 µm. (F) Quantification of Evans blue staining, comparing 14-day-old WT and *bfn1-1* roots. 10 plants were used for each genotype, taking four pictures along the main root axis per plant. ImageJ was used to calculate the mean grey value to compare relative staining intensity. Statistical significance was determined using an unpaired, two-tailed Student's t test before normalization (*** P<0.0001). (G) Representative Proteostat staining images of 10-day-old WT and *bfn1-1* root tips. Scale indicates 100 µm. (H) Quantification of Proteostat staining using 4 to 5 10-day-old WT and *bfn1-1* roots. Statistical analysis was performed via one-way ANOVA and Tukey's post hoc test before normalization (significance threshold: P ≤0.05).

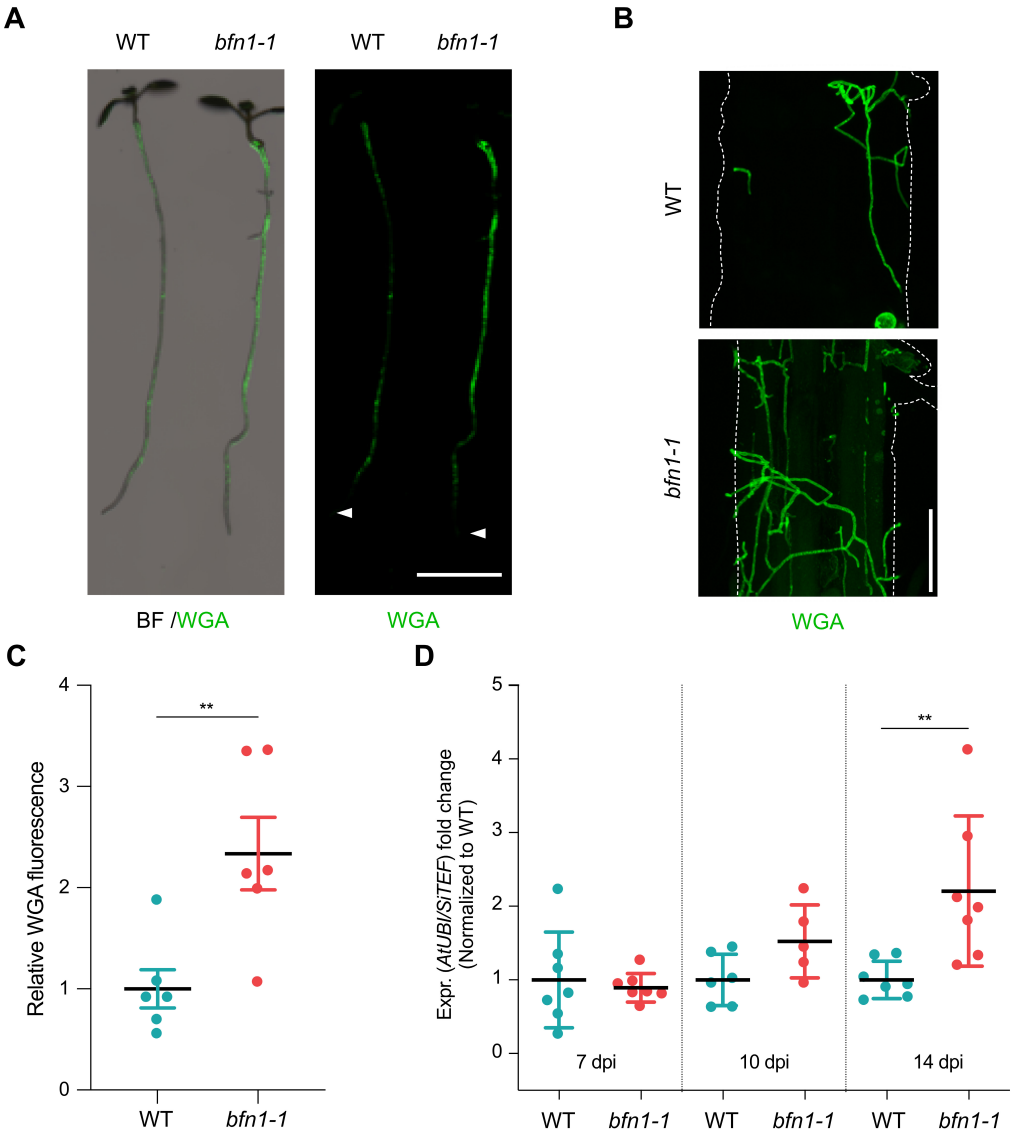

Figure 2. *bfn1-1* roots show increased colonization by *S. indica*. (A) Representative image showing extraradical colonization of 10-day-old WT and *bfn1-1* plants seed inoculated with *S. indica*. The fungus was stained with WGA-AF 488. Roots were scanned and captured with a LI-COR Odyssey M imager using the bright field (BF) and Alexa Fluor 488 channel. Arrowheads indicate the position of the root tips. Scale indicates 5 mm. (B) Representative images of Arabidopsis WT and *bfn1-1* roots inoculated with *S. indica* obtained by CLSM. The fungus was stained with WGA-AF 488. Scale represents 50 µm. (C) Relative quantification of WGA-AF 488 signal as a proxy for extra-radical colonization of *smb3* and WT roots. Statistical comparisons were made by unpaired, two-tailed Student's t test for unpaired samples (**$P < 0.01$) (D) Quantitative RT-PCR analysis to measure intraradical *S. indica* colonization in WT and *bfn1-1* roots. Roots were collected from 3 biological replicates, using approximately 30 plants per time point and replicate for each genotype. Each time point in the graph is normalized to WT for relative quantification of colonization. Statistical analysis was performed via one-way ANOVA and Tukey's post hoc test (significance threshold: $P \leq 0.05$).

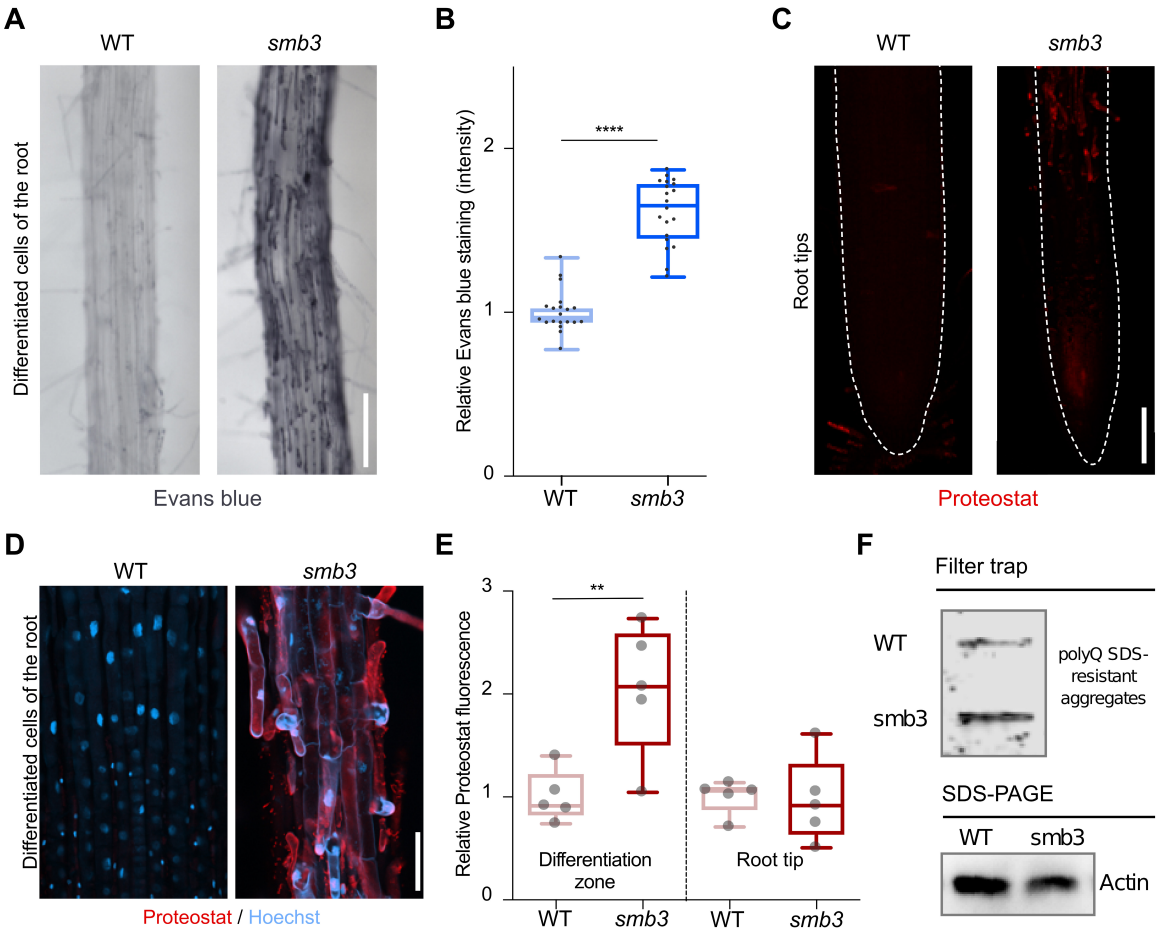

634

635 **Figure 3. *smb3* roots exhibit uncleared cell corpses loaded with misfolded/aggregated**
636 **proteins.** (A) Evans blue staining of the differentiation zone in 17-day-old WT and *smb3* roots**.**
637 Scale indicates 100 µm. (B) Relative quantification of Evans blue staining of the differentiation
638 zone in 14-day-old WT and *smb3* roots. Five plants per genotype were used, taking 4 images per
639 plant along the main root axis. Statistical relevance was determined by unpaired, two-tailed
640 Student's t test before normalization (**** P<0.0001). (C) Representative images of 10-day-old
641 WT and *smb3* roots stained with Proteostat (red). Scale indicates 100 µm. (D) Magnification of
642 the differentiation zone of WT and *smb3* roots. Proteostat (red) and Hoechst (blue) channels are
643 shown. Scale indicates 50 µm. (E) Quantification of relative Proteostat fluorescence levels
644 comparing the differentiation and meristematic zones of WT and *smb3*. 5 x 10-day-old plants were
645 used for each genotype. Statistical significance was determined by one-way ANOVA and Tukey's
646 post hoc test before normalization (significance threshold: P ≤0.05). (F) Filter trap and SDS-PAGE
647 analysis with antibody against poly-glutamine (polyQ) regions of 15-day-old WT and *smb3* roots.
648 The images are representative of two independent experiments.

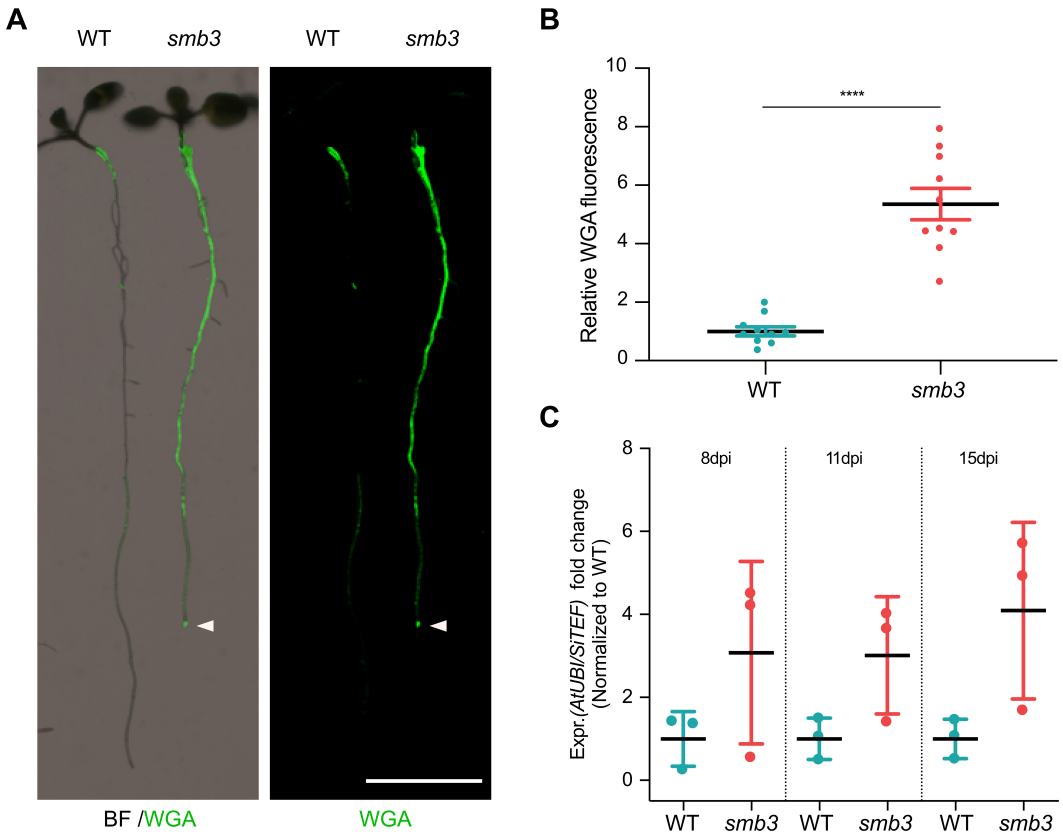

649

650 **Figure 4. *smb3* roots display increased intra- and extraradical colonization by *S. indica*.** (A)
651 Representative image showing extraradical colonization of 10-day-old WT and *smb3* seedlings
652 (seed inoculated). *S. indica* was stained with WGA-AF 488. Roots were scanned and captured
653 with a LI-COR Odyssey M imager using the bright field (BF) and Alexa Fluor 488 channel. White
654 arrowheads indicate colonization at the root tip in *smb3*. Scale indicates 5 mm. (B) Relative
655 quantification of WGA-AF 488 signal indicating extra-radical colonization on *smb3* and WT roots.
656 The statistical comparison was made by two-tailed Student's t test for unpaired samples (****$P <$
657 0.0001) using 10 plants. (C) Measurement of intraradical colonization in WT and *smb3* roots
658 performed by quantitative RT-PCR. Roots from 3 biological replicates were collected and washed
659 to remove extra-radical hyphae, using approximately 30 seedlings for each genotype per time
660 point and replicate. Each time point in the graph is normalized to WT for a relative quantification
661 of colonization. Statistical analysis was done via one-way ANOVA and Tukey's post hoc test after
662 normalization (significance threshold: $P \leq 0.05$).

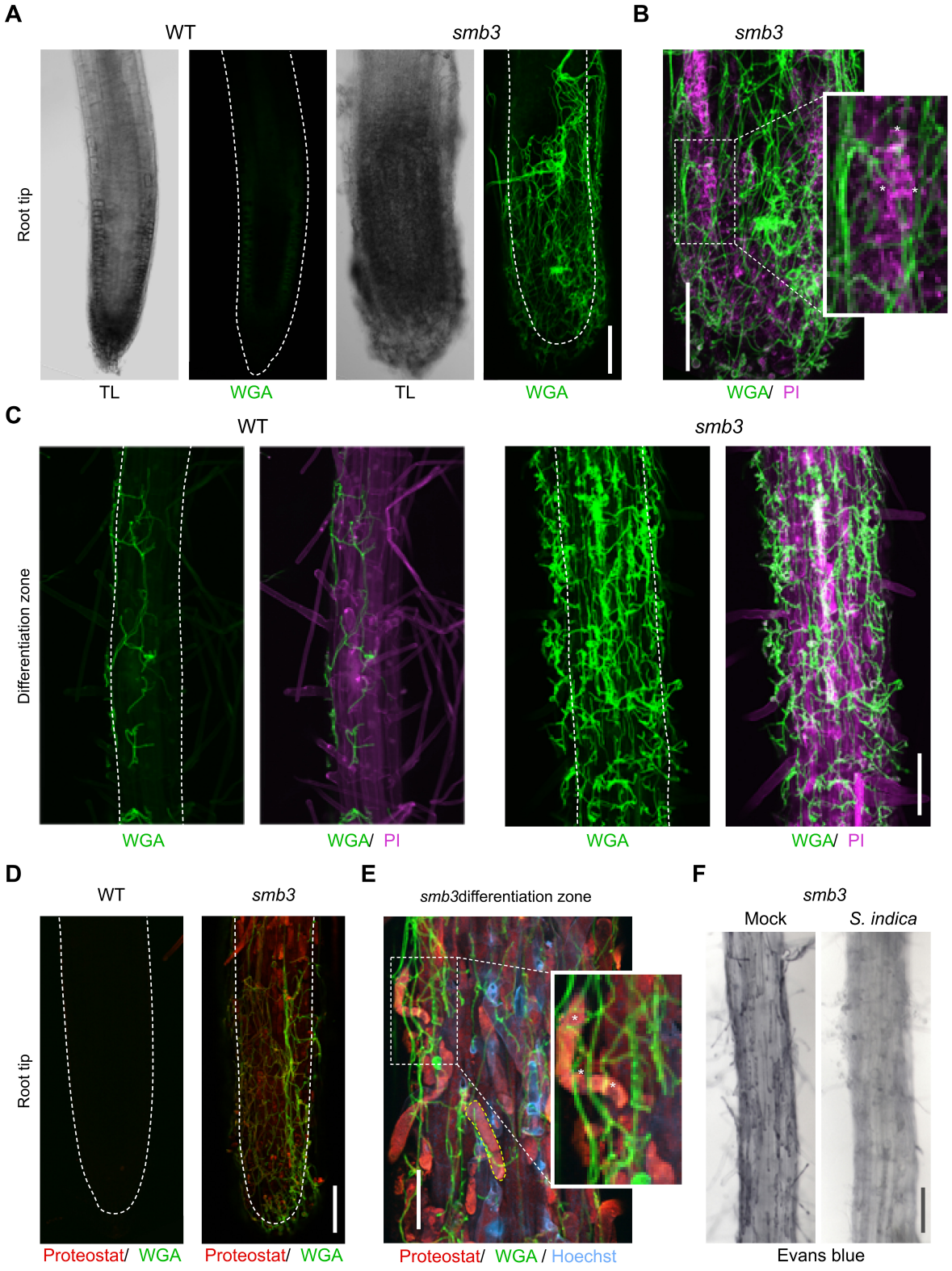

Figure 5. Cytological analysis of *S. indica*-colonized *smb3* and WT roots. For microscopic analysis, 7-day-old seedlings were inoculated with *S. indica* spores and the roots were analyzed at 10 dpi. (A) Representative images of Arabidopsis WT and *smb3* roots inoculated with *S. indica*.

667 *S. indica* was stained with WGA-AF 488. Transmitted light (TL) images are also shown. Scale
668 indicates 100 µm (B) Magnification of *smb3* root tip colonized with *S. indica*. Asterisks indicate
669 penetration of hyphae stained with WGA-AF 488 into dead cells stained with propidium iodide
670 (PI). Scale indicates 100 µm. (C) Representative images of WT and *smb3* roots colonized with *S.*
671 *indica* and stained with WGA-AF 488 and PI. Scale indicates 100 µm. (D) Representative images
672 of WT and *smb3* root tips inoculated with *S. indica* stained with WGA-AF 488 and Proteostat.
673 Scale indicates 100 µm (E) Magnification of *smb3* root differentiation zone showing *S. indica*
674 colonization stained with WGA-AF 488, Hoechst and Proteostat. Penetration of uncleared cell
675 corpses is marked with asterisks. Scale indicates 50 µm. (F) Evans blue staining showing sections
676 of the differentiation zone in *smb3* mock-treated and colonized roots with *S. indica* at 10 dpi**.** Scale
677 indicates 100 µm.

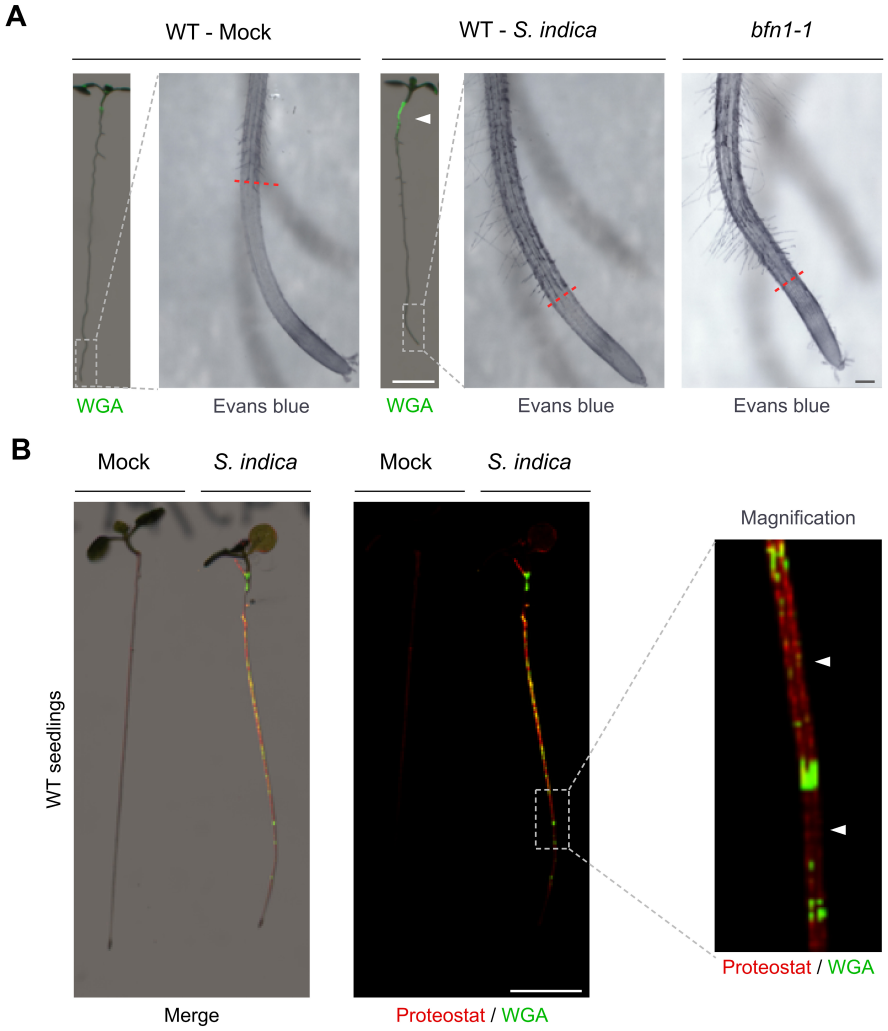

678

679 **Figure 6. *S. indica* causes a systemic cell death response in the root differentiation zones.**
680 (A) Comparison of WT and *bfn1-1* roots inoculated with *S. indica*. Representative scan images of
681 a whole plant taken with LI-COR and microscopy root tip overviews. The LI-COR scans of fungal
682 mycelium stained with WGA-AF 488 show a preference for the mature differentiation zone for
683 fungal colonization, indicated by a white arrowhead. Scale bar indicates 5 mm. Evans blue cell

684 death staining in WT-mock, WT-colonized, and *bfn1-1* roots. Cell death staining highlights a
685 pattern of dead cells in *S. indica*-colonized plants near the root tip in young differentiated tissue
686 as indicated with a dotted red line. Scale bar indicates 100 µm. (B) Representative Proteostat
687 images of *S. indica*-colonized WT roots. Magnification panel shows Proteostat staining in zones
688 of the root where *S. indica* is not present (white arrowheads). Scale indicates 5 mm.

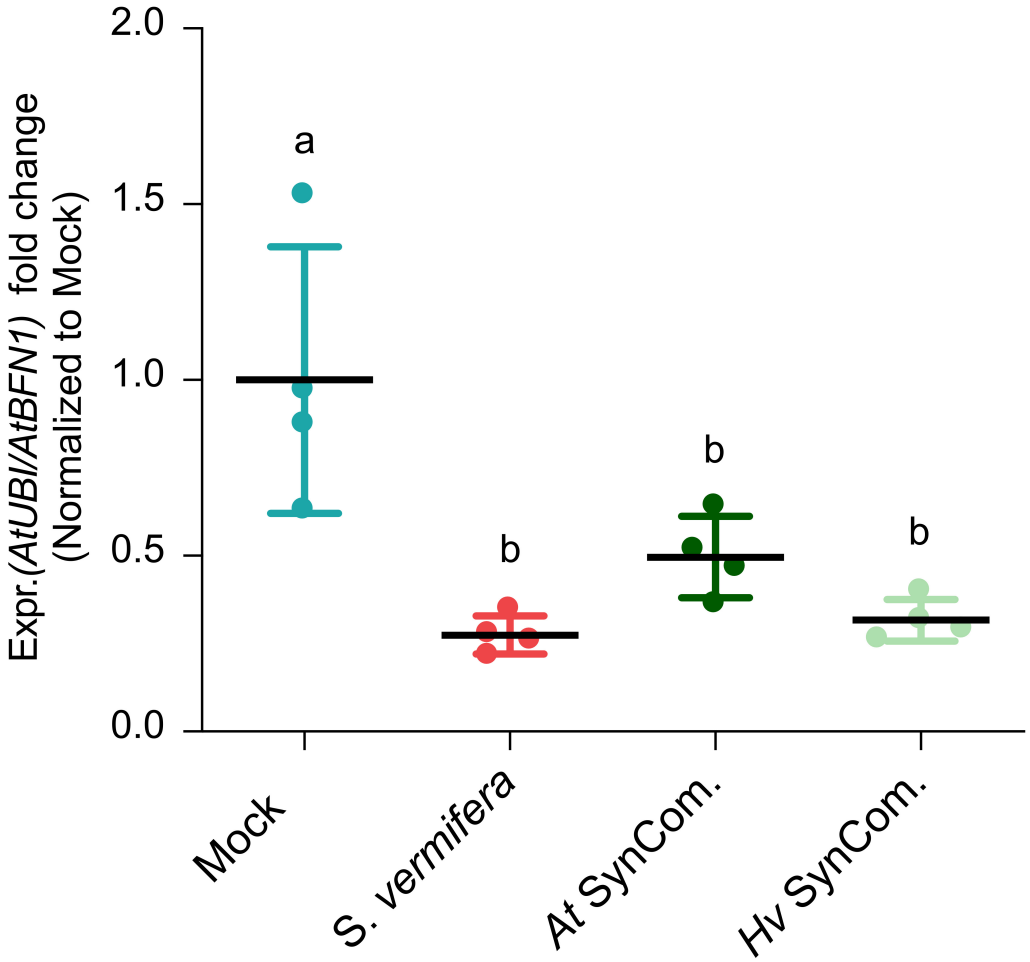

689

690 **Figure 7. *BFN1* is downregulated during colonization by beneficial microbes**. Quantitative
691 RT-PCR shows downregulation of *BFN1* in *A. thaliana* (*At*) during colonization by *S. vermifera*
692 and the *H. vulgare* (*Hv*) and *A. thaliana* synthetic bacterial communities (SynComs). RNA was
693 harvested from 4 replicates at 6 dpi using 30 plants per replicate for each treatment. *BFN1*
694 expression levels are normalized to mock conditions. Statistical evaluation was performed via
695 one-way ANOVA and Tukey's post hoc test before normalization (significance threshold: $P \leq 0.05$).

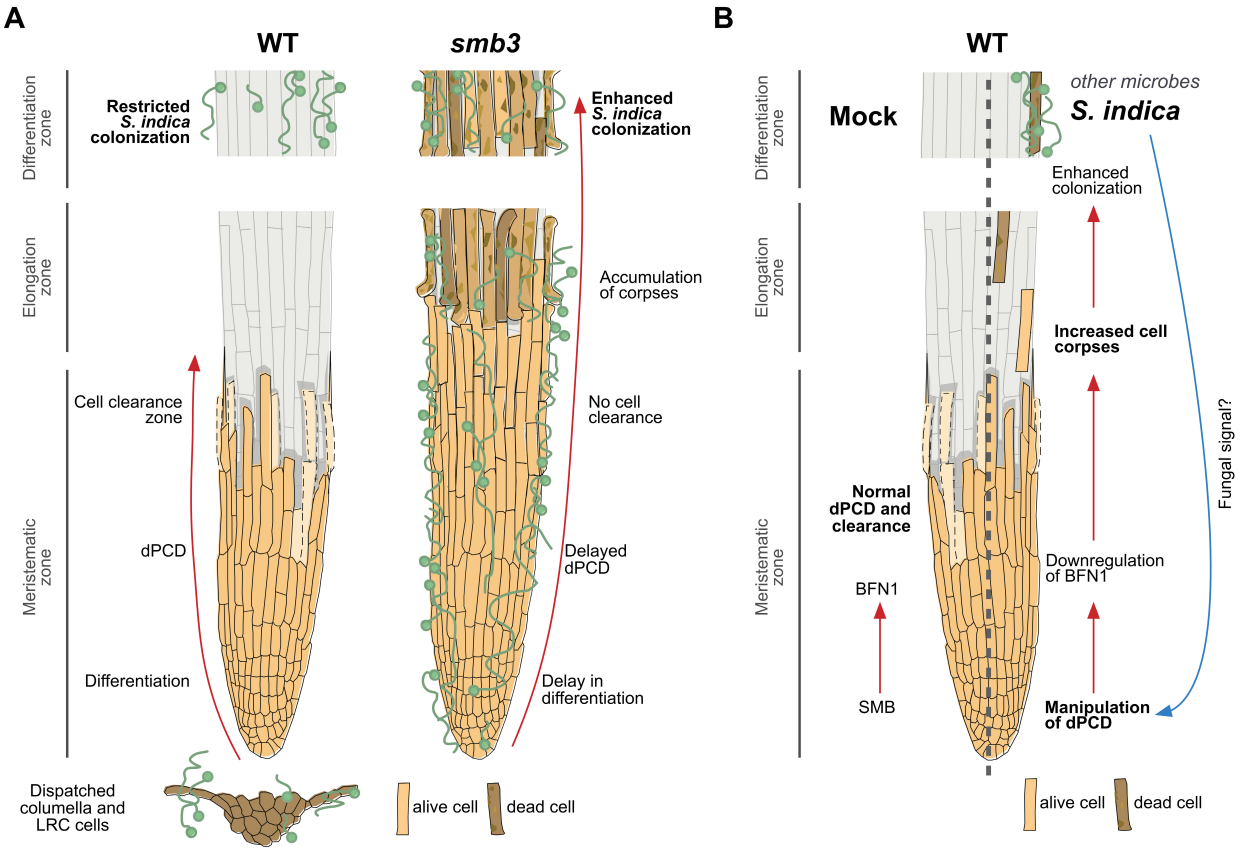

Figure 8. Proposed models for manipulation of dPCD and implications for the interaction with *S. indica*. (A) The size of the root cap organ in Arabidopsis is maintained by high cell turnover of root cap cells and cell corpse clearance. While the columella root cap is shed from the root tip, a dPCD machinery marks the final step of LRC differentiation and prevents LRC cells from entering the elongation zone. Induction of cell death by the transcription factor SMB is followed by irreversible DNA fragmentation and cell corpse clearance, mediated by the nuclease BFN1, a downstream component of dPCD (Fendrych et al., 2014). The absence of dPCD induction in the *smb3* knockout mutant leads to a delay in LRC differentiation and allows LRC cells to enter the elongation zone, where they die an uncontrolled cell death and remain attached to the root as dying cells or cell corpses. The *smb3* phenotype significantly enhances colonization of Arabidopsis by *S. indica*, as the fungus colonizes the entire root from the root tip to the differentiation zone and is not restricted to the differentiation zone as is the WT Arabidopsis roots. (B) *S. indica* manipulates dPCD in Arabidopsis roots by downregulating *BFN1*. We hypothesize that this leads to a reduced rate of cell corpse clearance in the root cap, which is beneficial for fungal colonization through increased nutrient availability in the form of dead LRC cells.